View metadata, citation and similar papers at core.ac.uk
brought to you by CORE
provided by RERO DOC Digital Library

Wood Sci Technol (2012) 46:333–347
DOI 10.1007/s00226-011-0404-4

ORIGINAL

Capacity prediction of welded timber joints

Till Vallée · Thomas Tannert · Christelle Ganne-Chedville

Received: 6 April 2010 / Published online: 16 February 2011
© Springer-Verlag 2011

Abstract Linear vibration welding of timber structural elements provides new opportunities to potentially achieve structural joints. This paper investigates to which extent welded joints can be considered for load-bearing structural joints. On the basis of a series of experimental and numerical investigations on a series of welded single-lap joints, failure modes were identified, and the associated failure criterion was quantified. A probabilistic method subsequently allowed accurately predicting the capacity of the tested wood welded joints exclusively based on objective input data, including an estimate of the scattering due to the material's inherent variability.

Introduction

Load-bearing timber joints

To connect load-bearing timber structures, practitioners have a series of methods at their disposal; some of them rely on mechanical fasteners (i.e., dowels), a second type of connections achieves load transmission by means of direct compressive or shear contact between timber members (i.e., dovetails), and a third increasingly considered option is adhesively bonding. It is less known that, besides the three above-listed classes of structural joints, a recently developed technique commonly labeled welding of wood also allows for load-bearing connections of timber elements. Welding of wood, as a quasi instantaneous joining technique, offers clear advantages over adhesively bonding, as the time needed for the adhesives to cure is one of the main drawbacks of adhesively bonded connections. The question to

T. Vallée (✉) · T. Tannert · C. Ganne-Chedville
Architecture, Wood and Civil Engineering, Bern University of Applied Sciences,
Solothurnstrasse 102, 2504 Biel, Switzerland
e-mail: till.vallee@fibreworks.org

which extent welded joints can be considered for load-bearing joints in structural timber engineering, and if so, how such joints can be dimensioned, remains open.

Welding of wood

Wood-to-wood connections by means of welding are an innovative process, which holds high potential for development, and research has just begun to investigate all aspects governing strength and durability of such connections. To achieve joints by means of welding of wood, the adherends are pressed against each other and rapidly vibrating heats up and melts the material at the interface within a few seconds. Once the motion stops, and after cooling down, a solid bond has formed (Ganne-Chédeville et al. 2008a). Since bonds are completed in less than a minute, and no further preparation of the surfaces is required, it is tempting to investigate potential structural applications (Leban et al. 2005).

First reports related to welding of wood date back to Sutthoff et al. (1996), subsequently, Gliniorz et al. (2001) pointed out that welding of wood holds potential for structural applications. Welding of wood based on linear vibration welding (LVW) greatly improves the homogeneity and resistance of the resulting bonds (Gfeller et al. 2004). LVW leads to a considerable increase in wood density in the welded overlap (Leban et al. 2004), which in turn results in melting processes of lignin and hemicelluloses, thus achieving a strong bond.

Two sets of parameters proved to have an influence on the bond strength: firstly, parameters related to the wood (Properzi et al. 2005; Stamm et al. 2005), i.e., species, year-ring orientation, moisture content, and density and size; and secondly, parameters related to the LVW device (Ganne-Chédeville et al. 2008a), i.e., amplitude and frequency of the vibration, friction pressure, and pressure duration.

Besides the above-mentioned mostly experimental works, finite element analysis (FEA) was used to simulate the temperature behavior during the welding process (Ganne-Chédeville et al. 2008b), with the aim to identify the influence of material parameters on the welding temperature. Besides thermal analysis, FEA proved to allow for a better insight in the mechanical behavior of wood welded joints: Oudjene et al. (2010) stands for a study on numerical modeling of butt joints connected by welded wood dowels under shear, where numerical and analytical results are in good agreement.

Capacity prediction of timber joints

The following issues have to be considered before addressing the question of capacity prediction of welded timber joint: (1) determining the stress–strain state in lap cemented joints, the term cemented crafted by Goland and Reissner (1944) being used herein as a generic term for adhesively bonded and welded joints and (2) identifying the failure mechanism of welded timber joints and quantifying the associated failure criterion. For reasons that will become clear when addressing (1)–(2), combined with the brittle nature of timber, makes it necessary to tackle (3) the question of size effects and its relation to material strength. Lastly, (4) it is paramount to implement (1)–(3) into an actionable capacity prediction routine.

The determination of stresses inside cemented joints has been first considered on a purely analytical basis, major milestones are Volkersen (1938) and Goland and Reissner (1944), followed by significant contributions by Hart-Smith (1974) and culminating in more recent publications by Tsai et al. (1998) and Zou et al. (2004); the short list not claiming to be exhaustive. Analytical formulae, however, are tributary to mechanical idealizations, i.e., isotropic and linear-elastic material properties. It is thus almost impossible to achieve an accurate estimate of stresses, when deviating from the latter, as it is the case with timber. To overcome the limitations of analytical models, FEA has proven to be particularly effective, as recently summarized by (Da Silva et al. 2009a, b).

Identifying the failure mechanism associated with cemented joints points out the materials, or interfaces, triggering the collapse, i.e., adhesive, cohesive, or adherend's failure, and thus defining joint capacity. Once the failure mechanism is identified, the focus can be set on quantifying the capacity. In the context of cemented joints, the stress state is characterized by a superposition of multiple stress components acting simultaneously, making it critical to consider their combined effect on material strength.

A number of failure criteria applicable to timber have been developed, and various in depth reviews were published, e.g., Kasal and Leichti (2005). A commonly applied criterion was proposed by Norris (1962), the latter being based on von Mises-Hencky distortion energy hypothesis; it basically corresponds to a Tsai-Hill formulation. Regarding failure criteria for interfaces, no such generalized theories exist, and investigations have to be carried out considering each individual case. Interphase failure, frequently associated with energetic failure criteria rather than being stress based, can also be tracked back to probabilistic concepts (Lamon 2001). Adding to the complexity of the matter, the associated experimental setups turn out to be quite complex.

Failure of timber, especially when submitted to tensile and shear stresses, can be characterized as being extremely brittle. Such failure is conceptually considered to be triggered by a single weak element, i.e., a defect, randomly distributed in the bulk material; thus the probability that such a defect is encountered in a structural element increases with its size. This is in essence the definition of size effects, which has been formalized by Weibull (1939), by offering a straightforward quantifiable relationship between the size of material samples and their respective failure strength. Since failure of cemented joints is usually associated with a combination of transverse tensile and shear stresses, it is paramount to consider size effects, when handling capacity prediction methods.

All above-developed considerations have to be integrated into a prediction method. It has been shown on several occurrences that any attempt to predict the capacity of cemented joints composed of brittle adherends using a stress-based metric is deemed to fail, i.e., for FRP adherends (Vallée et al. 2006a) and timber adherends (Tannert et al. 2010a). To overcome the problematic associated with the sharp stress peaks and the brittle nature of adherends, a probabilistic dimensioning method was successfully tested against experimental data (Vallée et al. 2006b; Tannert et al. 2010b). The method, besides yielding accurate predictions, offers an explanation for the increased material resistance toward steep stress gradients; it has

the additional benefit of relying solely on objective geometrical and mechanical parameters, excluding any empirical input.

Objectives

The objectives of this paper are threefold: (1) investigating to which extent welded joints can be considered for load-bearing structural joints, (2) identifying the failure modes and quantifying the associated criteria, and finally (3) presenting a method to accurately dimension structural wood welded joints by predicting its capacity exclusively based on objective input data, including an estimate of the scattering due to the material's inherent variability.

Experimental investigation

Material

In order to investigate the strength of wood welded connections, a series of single-lap welded timber joints was investigated in which the solely varied parameter was the overlap length, L. The timber species used was spruce (*Picea abies)* cut from high quality almost defect-free boards. The authors are aware that this leads to consider an idealized situation, since in practical applications such a selection is unlikely to occur. However, using less strictly selected timber will in first instance only increase the scattering of material strength, without altering the principles behind the dimensioning method subsequently developed.

Specimen description

Wood welded single-lap joints were manufactured using spruce by following a two-step process. First, two timber boards, 700 mm long, 60 mm in width, and 15 mm in thickness, were welded together by means of a Branson M-DT24L linear vibration welding machine (LVWM). A frequency of 100 Hz and an amplitude of 3 mm were applied. The parameters for spruce were previously optimized to a welding time of 10 s, holding time of 60 s, and pressure of 1.75 MPa. Since the purpose of this publication was not the discussion of the influence of the various manufacturing parameters on the strength of welded joints, they are just listed herein for the sake of comprehensiveness. The welded connections were manufactured in radial/tangential grain orientation (grain angles 45°). Subsequently, a grove up to the wood weld was cut in each of the now connected boards, the distance between the two groves defining the overlap length. The overlap length was varied from 100 to 400 mm in steps of 100 mm. The width and thickness of the adherends were kept constant with 60 and 15 mm, respectively; Fig. 1 details the used nomenclature. Each of the welded lap joints was manufactured, and subsequently tested, five times, to achieve a satisfactory level of statistical confidence.

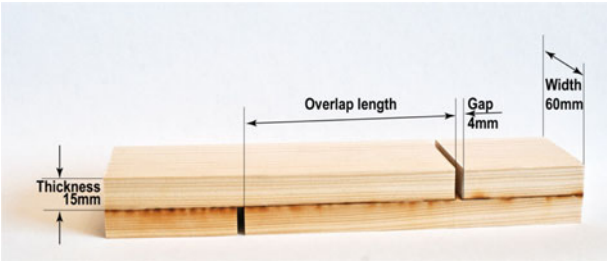

Fig. 1 Geometry of single-lap joint specimens (*not to scale*)

Characterization of the timber

The mechanical properties required for the numerical investigations (longitudinal and transverse modulus of elasticity E_X and E_Y) were determined on specimens cut from the same boards that were used to produce the joints. Table 2 summarizes the results; the elastic moduli range are at the high end of the values stated in the literature (Green et al. 1999), the difference is explained by the use of high quality almost defect-free timber.

The orthotropic mechanical properties of the timber, subsequently required for the numerical investigations, were determined on specimens cut from the same boards that were used to produce the joints, similar to the successfully applied procedure in previous investigations (Tannert et al. 2010a). This procedure yielded values for stiffness and strength in longitudinal, radial, and shear, listed below, which have to be seen in conjunction with the derived failure criterion, which is described by Eq. 1

$$\left(\frac{\sigma_x}{f_X}\right)^2 - \left(\frac{\sigma_X \sigma_Y}{f_X f_Y}\right) + \left(\frac{\sigma_Y}{f_{XY}}\right)^2 + \left(\frac{\tau_{XY}}{f_{XY}}\right)^2 = 1 \left(\frac{\sigma_Y}{f_Y}\right)^2 = 1 \left(\frac{\sigma_X}{f_X}\right)^2 = 1 \qquad (1)$$

where σ_X, σ_Y, and τ_{XY}, are the normal and shear stresses, respectively, and f_X, f_Y, f_{XY} are the material strength parameters. Herein, $f_X = 98.2$ MPa, $f_{XY} = 4.46$ MPa, and $f_{XY} = 13.7$ MPa, while $E_X = 17{,}910$ MPa and $E_Y = E_Z = 1{,}120$ MPa.

Characterization of the wood welded interface

Additionally to the aforementioned timber characterization, the authors determined the mechanical resistance of the wood welded interface. As detailed in the introduction, it is necessary to determine the strength with regard to simultaneously acting stresses, herein stresses parallel to the weld line, σ_X, perpendicular to the weld line, σ_Y, and shear stresses acting on the interface, τ_{XY}.

To experimentally handle the determination of the corresponding strength data in one consistent test-setup, it was decided to perform a series of off-axis tests. In a nutshell, the setup is an adaptation of the off-axis tests, as described in theory in Xavier et al. (2004), and exemplary implemented for the purpose of timber characterization in Tannert et al. (2010a): small samples of representative wood weld (cross-section 10 mm by 20 mm, length 80–120 mm, depending on the

considered off-axis angle) were carefully cut from the welded boards previously described, before the groves were driven-in.

The samples were cut in such a fashion that the wood weld exhibited an off-axis angle, α, with regard to the axis of the sample. Five different sets of off-axis angles were considered, ranging from $\alpha = 0°$ to 60° in steps of 15°. A subset of the resulting specimens is depicted in Fig. 2.

Tests on wood welded lap joints

The experiments on the wood welded single-lap joints were performed in UTM as quasi-static axial tensile tests under a displacement-controlled rate of 1 mm/s, up to failure load. The controlled laboratory conditions were kept constant at 22°C temperature and 65% relative humidity. For all specimens, the load displacement behavior was measured and recorded up to the maximum load (F_{ult}).

Analysis of variance (ANOVA) was carried out to evaluate the effect of the overlap length on F_{ult}. Based on the number of observations, a P value is calculated and compared to the significance level, α, typically chosen as >0.05. If the P value is smaller than α, then the hypothesis of no differences between means is rejected (Montgomery and Runger 2003).

Experimental results

The off-axis samples on the welded interface exhibited a similar almost linear load–displacement behavior, and failure occurred in the same brittle manner. Post-failure observation indicated that the manufacturing process did, for a significant fraction of samples, lead to insufficiently welded surfaces, as exemplary shown in Fig. 3. The latter effect involved the samples that resulted in the lower 10%-quantile strength of each individual sample set, defined by the corresponding off-axis angle; the corresponding data were thus discarded. The raw experimental result of the not rejected data is displayed in Table 1. Besides the mean values corresponding to each off-axis angle, two different metrics for the scattering were determined: the variance

Fig. 2 Welded wood specimens: small scale samples

Fig. 3 Failure of off-axis samples: (*left*) rejected and (*right*) not rejected

Table 1 Experimental results on off-axis samples

Off-axis angle α	0°	15°	30°	45°	60°
Number	60	49	55	49	48
Mean [MPa]	0.610	0.461	0.853	1.041	2.076
Variance	21%	38%	32%	44%	25%
Weibull modulus k	3.905	3.866	3.888	3.742	3.863
Characteristic stress σ_0	0.567	0.399	0.748	0.834	1.815

(which ranged from 21 to 44%), and the Weibull modulus (ranging from 3.74 to 3.91). This strength data resulting from the off-axis samples are subsequently post-processed to determine the failure criterion of the wood weld, refer to section "Strength of the investigated welded interface".

All wood welded single-lap joints exhibited almost perfectly linear-elastic load–displacement behavior, and failed in a brittle and sudden manner. A closer post-failure observation indicates that the welding process did not always yield perfectly welded surface, see Fig. 4. The experimental results are displayed in Fig. 5, where all individual test results are plotted against the overlap length. Table 2 lists the mean values, as well as variance (defined herein as the ratio of standard deviation to the means), as a metric for the scattering. It clearly appears that the capacity of the welded joints increases with overlap length, but that the increase is limited toward higher overlap lengths, indicating a critical overlap length, herein approx. 300 mm, beyond which no further increase in strength can be expected. Considering each series individually, i.e., resulting from five corresponding specimens of the same overlap length, it appears that scattering ranges between 21 and 35%; if considering the whole experimental program, variance amounts to 25%. Besides the mean values and the corresponding variances, the upper and lower 5%-quantile values were also determined; two different definitions thereof were considered and listed in Table 2: quantile values obtained based on the scattering inside each series, and quantile values based on the scattering of the experimental data from all overlap lengths.

Fig. 4 Failure of welded wood specimens

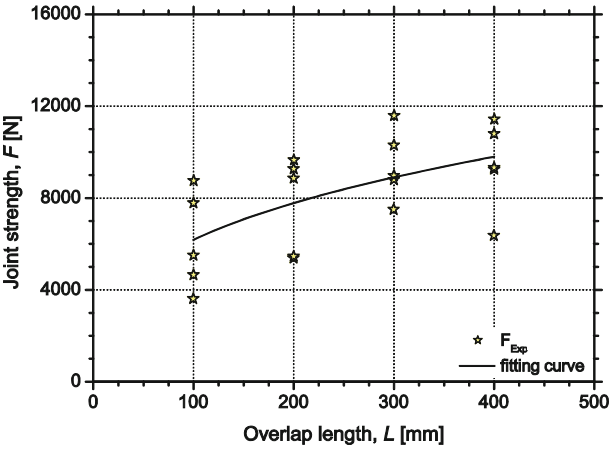

Fig. 5 Capacity of the wood welded single-lap joints versus overlap length

ANOVA at a level $\alpha = 0.05$ was applied to statistically evaluate the results. The overlap length has a significant effect on joint with $P = 0.044$. Multiple comparison tests (Least Square Differences at a level $\alpha = 0.05$) showed no significant differences in strength beyond 300 mm overlap.

Capacity prediction

Numerical model for wood welded single-lap joints

The determination of the stresses along the welded overlap line was achieved by means of numerical modeling, using the FEA package Ansys® (v13). Timber is an anisotropic and inhomogeneous material, but for simplicity in modeling, the

Table 2 Welded joint capacity data

Overlap [mm]	100	200	300	400
Experimental [N]	6,062	7,726	9,429	9,435
Standard deviation [N]	2,150	2,121	1,559	1,957
Variance [−]	35%	27%	17%	21%
Predicted load	5,344	6,129	8,025	8,852
Accuracy [−]	12%	21%	15%	6%
P value [−]	0.49	0.10	0.15	0.53
Experimental 5%-quantile per series [N]	2,532	4,256	6,852	6,232
Experimental 5%-quantile all series [N]	2,874	3,856	4,706	4,709
Predicted 5%-quantile [N]	2,402	2,753	3,605	3,977
Accuracy related to series [−]	5%	35%	47%	36%
Accuracy related to full series [−]	16%	29%	23%	16%
Experimental 95%-quantile per series [N]	9,578	11,208	11,992	12,638
Experimental 95%-quantile all series [N]	9,251	11,789	14,389	14,397
Predicted 95%-quantile [N]	8,369	9,597	12,567	13,862
Accuracy related to series [−]	13%	14%	−5%	−10%
Accuracy related to full series [−]	10%	19%	13%	4%

material was assumed to be homogeneous and transverse orthotropic with identical properties in radial and tangential directions. The longitudinal direction is referred to as parallel to grain (herein defined by the subscript X), while the combined radial and tangential directions are referred to as perpendicular to grain (subscript Y). Previous studies (Vallée et al. 2006a; Tannert et al. 2010a) showed that 2D instead of 3D modeling of adhesively bonded joints is accurate enough, thus 2D 8-node orthotropic elements were used; a relatively tight mesh was applied (element size 1 mm), which was further refined at the locations where stress concentrations occurred. The timber was modeled according to the mechanical data listed in 2.3. Following the experimental observations, the wood weld was modeled as being fully rigid; thus no specific interface elements were inserted. The computed transverse tensile stresses (perpendicular to the grain), σ_Y, and in-plane shear stresses, τ_{XY}, are plotted along the overlap length for all investigated overlap lengths, L, in Figs. 6 and 7.

Strength of the investigated welded interface

For the off-axis samples, the tensile load, *P*, results in stresses in the principal material axis (1, 2) by transformation as follows:

$$\sigma_X = \sigma_0 \cdot \cos^2 \alpha \quad \sigma_Y = \sigma_0 \cdot \sin^2 \alpha \quad \tau_{XY} = \sigma_0 \cdot \sin \alpha \cdot \cos \alpha \tag{2}$$

where $\sigma_0 = P/A$, A being the cross-sectional area of the specimen and α the off-axis orientation related to the weld line. For each sample, the acting stress, σ_0, has to be transformed into the corresponding σ_X, σ_Y, and τ_{XY} using (Eq. 2), which act simultaneously.

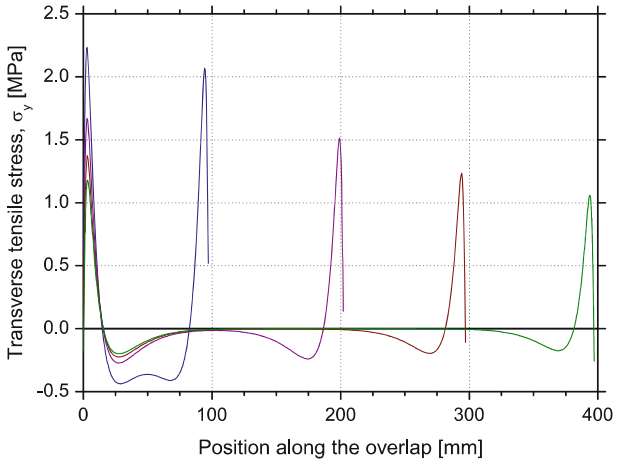

Fig. 6 Tension perpendicular to the grain stresses, σy, for a reference load of $F = 10$ kN for four investigated overlap lengths

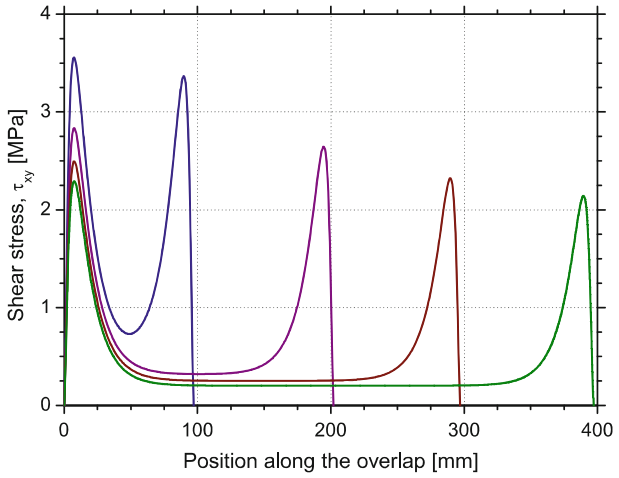

Fig. 7 Shear stresses, τxy, for a reference load of $F = 10$ kN for four investigated overlap lengths

Following a similar failure criteria formulation as for timber (Eq. 1), it can be shown that the influence of the longitudinal, σ_X, is almost negligible. By means of a subsequent statistical analysis, it was found that the off-axis data are best modeled by Eq. 3

$$\phi_W^2 = \left(\frac{\sigma_Y}{f_{W,Y}}\right)^2 + \left(\frac{\tau_{XY}}{f_{W,XY}}\right)^2 = 1 \tag{3}$$

where the parameters $f_{W,Y} = 0.61$ MPa and $f_{W,XY} = 1.07$ MPa representing the strength toward tensile out-of-plane stresses, respectively, the shear strength. Since the off-axis samples exhibited systematic brittle failure, it was decided to achieve

the statistical modeling of the latter by a Weibull distribution, see Eq. 4, which has proved to be the most accurate approximation for such failure type.

$$P_s = \exp\left[-\int_V \left(\frac{\sigma}{\sigma_0}\right)^k \mathrm{d}V\right]. \tag{4}$$

In Eq. 4, P_s is the probability of survival corresponding to the stress σ acting over a volume V, σ_0 is the characteristic stress or scale parameter, and k is the shape parameter that gives a measure of the strength variability, with low values of k corresponding to a high variability. One consequence of Eq. 2 is that for two sizes S_1 and S_2 submitted to constant stresses σ_1 and σ_2 at failure, assuming equal probabilities of survival, the relationship given in Eq. 5 is obtained:

$$\frac{\sigma_1}{\sigma_2} = \left(\frac{S_2}{S_1}\right)^{1/k}. \tag{5}$$

The quantity size, labeled herein S_i, being either a length, an area, or a volume.

Determination of the Weibull parameters

As welded joints fail under a combination of stresses, it is necessary to extend the concept of the Weibull distribution toward stresses acting simultaneously. Since, following Eq. 3, $\phi_W^2 = 1$ defines failure, it was decided to (1) use the expression ϕ_W as a stress operator and subsequently (2) express all experimental results resulting from the off-axis samples, disregarding their respective off-axis angle α, accordingly. The corresponding statistical parameters, i.e., k and σ_0, were estimated using the least squares/rank regression method, Fig. 8, and yielded $k = 3.68$, respectively, $\sigma_0 = 1.15$.

Algorithm of joint capacity prediction

If the whole joint is idealized as being constituted by n elements, its survival depends on simultaneous non-failure of all elements. Consequently, if each constituent element i, with a volume A_i is subjected to $\sigma_{F,i}$, the probability of survival of the joint is given by:

$$P_S = \prod_{i=1}^{n} \exp\left[-\frac{A_i}{A_0}\cdot\left(\frac{\sigma_{F,i}}{\sigma_{F,0}}\right)^m\right] = \exp\sum_{i=1}^{n}\left[-\frac{A_i}{A_0}\cdot\left(\frac{\sigma_{F,i}}{\sigma_{F,0}}\right)^m\right] \tag{6}$$

where A_i are the areas of the considered surface elements constituting the overlap, A_0 is the area of the wood welded areas that failed in the off-axis samples, $\phi_{W,i}$ is given by (Eq. 3), σ_0 is the characteristic stress, and k is the shape parameter according to Eq. 4. As stated previously, the stresses σ_X, σ_Y, and τ_{XY}, needed to formulate ϕ_W, were gathered using FEA. Thus, after having determined all stresses, element by element, all $\phi_{W,i}$ were computed using a spreadsheet, and eventually the corresponding probability of failure, P_S, is associated with each element. The global

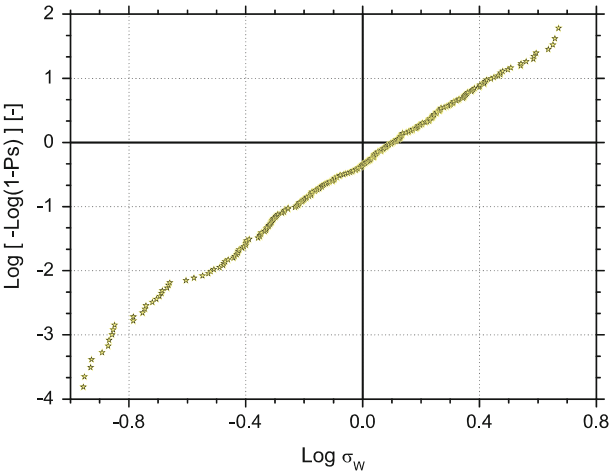

Fig. 8 Weibull plot of all off-axis samples

failure is thus defined as the load level, $F_{\mathrm{FEA.}}$, for which (Eq. 6) delivers a global probability of survival, P_{S}, equal to 50%.

Results of joint capacity prediction

The above-described probabilistic method was used to determine the strength of all investigated joint configurations. Besides the prediction of the mean values, which correspond to the above-mentioned 50%-quantile, the upper and lower 5%-quantile values are determined and plotted in Fig. 9 and listed in Table 2. The joint strengths as predicted using the probabilistic method increase almost linearly with the overlap length up to $L = 160$ mm, beyond which the strength increase flattens asymptotically for the joints.

Table 2 and Fig. 4 also compare the predicted capacities to the experimentally determined values; good agreement was obtained. In addition to F_{EXP} and F_{FEA}, Table 2 shows the deviation between these two values and the results of t-tests for the hypothesis: $F_{\mathrm{EXP}} = F_{\mathrm{FEA}}$. This hypothesis is rejected for those cases were the P-value is smaller than $\alpha = 0.05$ (95% significance level). For all joint capacities predicted using the probabilistic method, these hypotheses are accepted.

Discussion

Experimental results

Capacity of the welded single-lap joints is clearly positively correlated to the overlap length; however, it exhibits a similar tendency to a flattening beyond a critical overlap, herein at around 300 mm, like the one observed for adhesively bonded joints (Vallée et al. 2006a; Tannert et al. 2010a). The joint capacity is thus

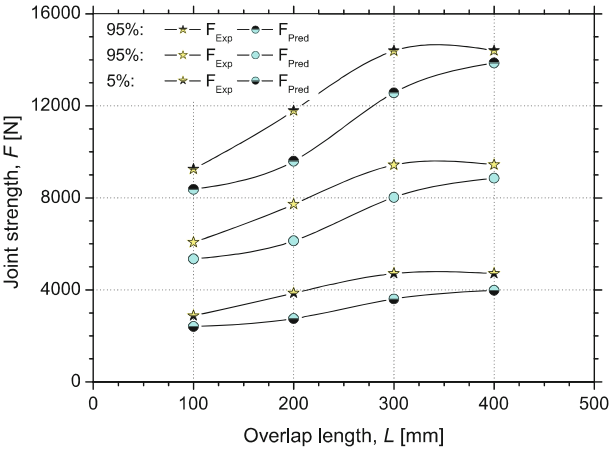

Fig. 9 Experimental versus predicted joint capacities: 5, 50, and 95% quantile values

limited to a value below roughly 12 kN. If considering that the welded timber members (60 × 15 mm with the determined strength), would only break at 89 kN, it becomes evident that welded joints are not very effective as a joining technique, since they achieve a joint efficiency of roughly 13%. Beyond that, welded joints exhibit very significant scattering, herein 25% on average, which leads to a very small lower 5%-quantile, often used as characteristic value for dimensioning procedures in engineering. It is clear, however, that a part of the unsatisfactory structural performance results from the fact that single-lap joints are *per se* not as effective, if compared to double lap joints.

Considering the off-axis tests, performed to determine the failure criterion of the welded interface, it must be emphasized that the suggested test-setup allowed for a straightforward experimental characterization. The results show the clear dependency of strength and off-axis angle. The scattering, if expressed by means of a normal distribution, i.e., defining the latter by variance, appears to be very significant (around 32% on average, up to 44% for $\alpha = 45°$). If, on the other hand, describing the scattering by means of a Weibull distribution, the scattering, then expressed by the value of the Weibull modulus k, the data are much more consistent: 3.85 ± 0.06; the latter rightly confirming that brittle failure is much better described using a Weibull distribution than a normal one.

Numerical results

The computed stress profiles along the overlap show the steep stress gradients typical for cemented joints. When considering increasing overlap lengths, it appears that the stress maxima tend to decrease. At comparable loads, and considering an overlap of 400 mm, tension perpendicular stresses amount for roughly half, shear stresses for around 64%, if compared to the specimen with an overlap of 100 mm. Correspondingly and on average, capacity for $L = 400$ mm increased by 44% compared to strength for $L = 100$ mm. Thus, the stress reductions associated with

increasing overlaps are consistent with the experimental evidence on joint capacities. However, it becomes also clear that in all cases, at failure, stress peaks do exceed the experimentally determined material resistance values (on average by around 150%) confirming that a stress-based method will not yield accurate strength predictions.

Capacity prediction

If considering size effects, as implemented in the probabilistic prediction routine, joint capacities are computed that match the experimental data, both considering the trend and the magnitudes, as indicated in Table 2 and graphically reported in Fig. 9. It appears that, on average, capacities are slightly underestimated by 13%. Because of the high scattering in experimental data, two subsequent comparisons, at the upper and lower 5%-quantile values, were also performed, and subsequently listed in Table 2 and Fig. 9: both indicate similarly good agreements (deviations of 21 and 11% on average, respectively). The good agreement at the quantile values sets the basis for characteristic design values in engineering applications.

Conclusions

Welding of wood was investigated in the light of application as a structural joint technique. Experimental and numerical investigations were carried out on a series of wood welded single-lap joints, in which the overlap length was varied. The resulting capacities, besides exhibiting large variability, were relatively low, if compared to the load capacity of the members.

Subsequently, the mechanical resistance of the welded connection was experimentally investigated using an adapted off-axis test. The latter relatively simple test-setup allowed characterizing the failure criterion. The experimental evidence confirmed the large variability of the strength of welded bonds, which turned out to be best described using Weibull statistics. The numerical results show that the load transfer in wood welded joints is conceptually comparable to adhesively bonded joints, i.e., steep stress profiles with the associated stress peaks. Lastly, a probabilistic joint strength method allowed to accurately predict the experimental mean values (on average by 13%), besides accurately quantifying the inherent variability (on average by around 16%), thus validating the method.

References

Da Silva LFM, Das Neves PJC, Adams RD, Spelt JK (2009a) Analytical models of adhesively bonded joints–Part I: literature survey. Int J Adhesion and Adhesives 29(3):319–330

Da Silva LFM, Das Neves PJC, Adams RD, Wang A, Spelt JK (2009b) Analytical models of adhesively bonded joints–Part II: comparative study. Int J Adhesion and Adhesives 29(3):331–341

Ganne-Chédeville C, Properzi M, Leban JM, Pizzi A, Pichelin F (2008a) Wood welding: chemical and physical changes according to the welding time. J Adhesion Sci Technol 22(7):761–773

Ganne-Chédeville C, Duchanois G, Pizzi A, Leban JM, Pichelin F (2008b) Predicting the thermal behaviour of wood during linear welding using the finite element method. J Adhesion Sci Technol 22(12):1209–1221

Gfeller B, Zanetti M, Properzi M, Pizzi A, Pichelin F, Lehmann M, Delmotte L (2004) J. Adhesion Sci Technol 17:1573–1589

Gliniorz KU, Mohr S, Natterer J, Navi P (2001) Wood welding. In: Proceedings of the 1st international conference of the European society for wood mechanics, Lausanne, Switzerland, pp 571–574

Goland M, Reissner E (1944) The stresses in cemented joints. J Appl Mech 29 (Trans. ASME) 11:A17–A27

Green DW, Winandy JE, Kretschmann DE (1999) Mechanical properties of wood. In: Wood handbook—wood as an engineering material. Forest Products Laboratory, Madison

Hart-Smith LJ (1974) Analysis and design of advanced composite bonded joints. Accession Number: 74N20564, Document ID: 19740012451, Report Number: NASA-CR-2218

Kasal B, Leichti RJ (2005) State of the art in multiaxial phenomenological failure criteria for wood members. Prog Struct Eng Mater 7(1):3–13

Lamon J (2001) A micromechanics-based approach to the mechanical behavior of brittle-matrix composites. Compos Sci Technol 61(15):2259–2272

Leban J-M, Pizzi A, Wieland S, Zanetti M, Properzi, Pichelin F (2004) X-ray microdensitometry analysis of vibration-welded wood. J Adhesion Sci Technol 18:673–685

Leban JM, Pizzi A, Properzi M, Pichelin F, Gelhaye P, Rose C (2005) Wood welding: a challenging alternative to conventional wood gluing. Scand J For Res 20:534–538

Montgomery DC, Runger GC (2003) Applied statistics and probability for engineers. Wiley, New York

Norris CB (1962) Strength of orthotropic materials subjected to combined stresses. Report No. 1816. Forest Products Laboratory, Madison

Oudjene M, Khelifa M, Segovia C, Pizzi A (2010) Application of numerical modelling to Dowel-Welded wood joints. J Adhesion Sci Technol 24(2):359–370

Properzi M, Leban JM, Pizzi A, Wieland S, Pichelin F, Lehmann M (2005) Influence of grain direction in vibrational wood welding. Holzforschung 59(1):23–27

Stamm B, Natterer J, Navi P (2005) Joining wood by friction welding. Holz Roh- Werkst 63:313–320

Sutthoff B, Franz U, Hentschel H, Schaaf A (1996) Verfahren zum reibschweissartigen Fügen und Verbinden von Holz. Patentschrift DE 196 20 273 C2, Deutsches Patent- und Markenamt

Tannert T, Vallée T, Hehl S (2010a) Probabilistic design of adhesively bonded timber joints, part I: experimental and numerical investigations. Submitted to Wood Sci Technol

Tannert T, Vallée T, Hehl S (2010b) Probabilistic design of adhesively bonded timber joints, part II: strength prediction. Submitted to Wood Sci Technol

Tsai MY, Oplinger DW, Morton J (1998) Improved theoretical solutions for adhesive lap joints. Int J Solids Struct 35(12):1163–1185

Vallée T, Correia JR, Keller T (2006a) Probabilistic strength prediction for double lap joints composed of pultruded GFRP profiles–Part I: experimental and numerical investigations. Compos Sci Technol 66(13):1915–1930

Vallée T, Correia JR, Keller T (2006b) Probabilistic strength prediction for double lap joints composed of pultruded GFRP profiles–Part II: strength prediction. Compos Sci Technol 66(13):1915–1930

Volkersen O (1938) Nietkraftverteilung in zugbeanspruchten konstanten Laschenquerschnitten. Luftfahrtforschung 15:41–47

Weibull W (1939) A statistical theory of strength of materials. In: Proceedings of the Royal Swedish Institute. Research No. 151, Stockholm, Sweden

Xavier JC, Garrido NM, Oliveira M, Morais JL, Camanho PP, Pierron F (2004) A comparison between the Iosipescu and off-axis shear test methods for the characterization of pinus pinaster ait. Compos Part A: Appl Sci Manuf 35(7–8):827–840

Zou GP, Shahin K, Taheri F (2004) An analytical solution for the analysis of symmetric composite adhesively bonded joints. Compos Struct 65(3–4):499–510